Received 24 May 2023; revised 26 July 2023 and 15 September 2023; accepted 29 September 2023. Date of publication 9 October 2023; date of current version 24 October 2023. Recommended by Senior Editor Sonia Martinez.

Digital Object Identifier 10.1109/OJCSYS.2023.3322906

Training Reflexes Using Adaptive Feedforward Control

ERICK MEJIA UZEDA (Graduate Student Member, IEEE), AND MIREILLE E. BROUCKE (Member, IEEE)

Electrical and Computer Engineering, University of Toronto, Toronto, ON M5S 1A1, Canada

CORRESPONDING AUTHOR: MIREILLE E. BROUCKE (e-mail: broucke@control.utoronto.ca)

This work was supported by the Natural Sciences and Engineering Research Council of Canada.

ABSTRACT We consider the problem of mixed feedforward and feedback based disturbance rejection, where the feedforward measurement only provides a partial reconstruction of the disturbance. In doing so, we pose a new biologically relevant disturbance rejection problem which puts the role of feedforward measurements at the forefront. Based on the architecture of the human brain, we propose a design that utilizes an adaptive internal model operating on a fast timescale that, in turn, trains the correct feedforward gains on a slow timescale. As such, the training of reflexes in biological systems can be explained by leveraging the theory of adaptive feedforward control. It is proven that our design provides an arbitrary level of disturbance attenuation, and the benefits of using reflexes are illustrated via a multitude of simulations.

INDEX TERMS Adaptive control, averaging analysis, disturbance rejection, feedforward control, systems neuroscience.

I. INTRODUCTION

The problem of *adaptive feedforward disturbance rejection* or *adaptive feedforward cancellation* has been widely studied in the control literature, both with known disturbance frequencies [1], [2], [3], [4] and unknown frequencies [5], [6]. These methods aim to reconstruct the *full* disturbance so that it can be cancelled using feedforward control. Closely related are methods based on the internal model principle [1], [2], [7], [8]. Applications include active vibration control in buildings [9]; robotics [10]; motor control in neuroscience [11]; active noise control [12], [13], [14], [15]; vibration control [16], [17]; disk drives [18]; marine systems [19]; wind turbines [20]; and many others.

A problem that has not been studied, to our knowledge, is one where the system is equipped with sensors that provide direct measurements of only a subset of components of the full disturbance. The presence of unmeasured disturbance components implies that one must incorporate additional disturbance rejection modules. A naive design would be to simply ignore sensory measurements, allowing an adaptive internal model to take over all work of disturbance rejection. The downsides of the naive approach are several: higher computational cost, slower response, and perhaps most egregious, reduced efficacy to cancel brief (not persistent) disturbances. We seek a design in which sensory measurements of disturbances work in tandem with adaptive internal models for enhanced disturbance rejection capabilities. In particular, we study the case when partial disturbance measurements with the correct phase and frequencies are available, but the amplitude of their contribution to the disturbance is unknown.

At the heart of the mixed adaptive internal model / feedforward control problem lies one of the central challenges of adaptive control: the management of persistent excitation to achieve parameter convergence. The key issue is that feedforward control inputs usurp excitation from other adaptive processes such as adaptive internal models. They present themselves in the form of *redundant regressors*, competing for available excitation. If the overall system is not properly architected, parameter convergence will not, in general, be guaranteed. In turn, if feedforward control amplitudes are not properly adapted, the utility of feedforward control is undermined.

Our motivation for studying feedforward control in disturbance rejection problems stems from systems neuroscience: the brain utilizes thousands of adaptive feedforward *reflex* inputs to achieve near instantaneous disturbance rejection of measurable components of disturbances, a feat impossible to achieve using more complex algorithms such as adaptive

internal models. How the brain coordinates and calibrates all these reflex signals has been the subject of intensive investigation in neuroscience for the last 60 years [11].

Related Work: The study of adaptive feedforward control for the purpose of disturbance cancellation appears to originate in [21] and has subsequently proliferated in the control literature, with only a small subset highlighted here. The variants of the problem may be classified according to the information available: the amplitude, phase, or frequencies of the disturbance may be known or unknown; and the plant may be known or uncertain. A clear trend of recent literature is to strip away as many assumptions on a priori information [22], [23]. However, almost all previous literature considers only one disturbance rejection module in operation. For example, if a direct measurement of the disturbance is available, then an internal model would not be used. The more realistic case of partial disturbance measurements working in tandem with other disturbance rejection modules has largely been overlooked, despite the prevalence of this case in robotics [24] and neuroscience [11]. An exception is [7] which presents both a feedback and feedforward controller to achieve perfect regulation. A caveat of their design is that the feedforward term is only useful for disturbance rejection when the initial condition of the exosystem is exactly known, contrasting with our problem. Also, robustness to brief disturbances is not considered.

Recent literature on over-modelled internal models [8], [25] contends with issues related to our work, namely managing lack of persistent excitation due to the possibility of redundant regressors. The paper [25] shows that a reduced set of parameters of the adaptive internal model associated with a reduced exosystem always converges to their correct values, despite a lack of excitation. The paper [8] deals with redundant regressors by directly monitoring the level of excitation in regressors. These methods adapt all parameters simultaneously such that the redundancy in regressors impedes parameter convergence. Instead, we show this problem can be mitigated by pushing downstream the excitation from one disturbance rejection module to another through a separation of timescales. This architectural intervention helps disambiguate the parameters that must be recovered.

The goal of the present work may also be contrasted with [1], in which a known linear time-invariant (LTI) plant is perturbed by sinusoidal disturbances for which a certain number of frequencies are known, but the amplitudes and phases are unknown. The authors show that higher-order harmonics can be partially attenuated using an adaptive feedforward control scheme designed to cancel known frequency components. The method was extended to the nonlinear setting in [26], where averaging analysis and semi-global stabilization techniques were applied to formalize the findings; see also [2]. In this article we consider disturbances with arbitrary (sinusoidal) measured and unmeasured components, not only higher-order harmonics; and we seek full attenuation of the overall disturbance on a fast timescale. Further, we emphasize the relationship between the feedforward controller and the internal model: the feedforward control should reduce the work of the internal model to the extent possible.

The present investigation is an outgrowth of our work on modeling the cerebellum using adaptive internal models [27], [28]. There we considered adaptive processes housed in the cerebellum for the purpose of short-term disturbance rejection. Particularly, we assumed that all reflex gains (known to be adapted slowly) are constants. The present work removes the restriction of constant reflex gains, thereby bringing the true two timescale behavior into view.

Contributions: In Section II we present a new biologically motivated disturbance rejection problem that puts feedforward measurements at the forefront of the disturbance rejection process. In Sections III-A and III-B we present a two timescale update law for the adaptation of feedforward gains inspired by the Miles-Lisberger hypothesis [29]. In Section III-C we begin by presenting an explicit converse Lyapunov function for linear time-varying systems appearing in adaptive control to reduce averaging analysis to standard Lyapunov arguments. Then we detail an iterative Lyapunov stability analysis, comprising Lemma 3 and Theorems 1–2, that culminates in showing that the proposed design achieves an arbitrary level of disturbance attenuation of $\mathcal{O}(\varepsilon)$ for all $\varepsilon > 0$ sufficiently small. Moreover, we have asymptotic disturbance rejection if there is no unmeasurable component of the disturbance. We also show that our proposed design disambiguates adapted parameters by de-correlating the unmeasured disturbance from the feedforward measurement.

Section IV demonstrates the usefulness of our design through two examples. We first present a third-order pedagogical example to demonstrate that standard adaptive control methods fail to meet the specifications of our disturbance rejection problem, while the proposed design gives reasonable performance. The second example from systems neuroscience regards long-term adaptation of the vestibuloocular (VOR) gain. A brief qualitative description of the Miles-Lisberger hypothesis allows the reader to apprehend how it informed our design. We consider three standard behaviors associated with VOR adaptation, demonstrating that our design is biologically plausible to capture cerebellar-brainstem interactions predicted by the Miles-Lisberger hypothesis.

II. PROBLEM STATEMENT

For the sake of exposition, we study a single-input LTI system in matched disturbance form

$$\dot{x} = Ax + Bu - Bd \tag{1a}$$

$$\dot{\zeta} = S\zeta \tag{1b}$$

$$d = \Gamma\zeta\,. \tag{1c}$$

where $x(t) \in \mathbb{R}^n$ is the state, $u(t) \in \mathbb{R}$ is the input, $\zeta(t) \in \mathbb{R}^q$ is the exosystem state, and $d(t) \in \mathbb{R}$ is a bounded disturbance. Suppose we have a *sensory measurement* $y(t) \in \mathbb{R}^p$ of disturbances (y is not a state measurement). To remain consistent with the LTI systems framework studied in the article, we

assume y is generated by LTI exosystems

$$\dot{\zeta}_i = S_i \zeta_i \tag{2a}$$

$$y_i = \Gamma_i \zeta_i \,, \tag{2b}$$

where $\zeta_i(t) \in \mathbb{R}^q$ for $1 \leq i \leq p$, and y_i is the i-th component of y. The assumption that S and S_i have the same dimension is wlog; see Remark 1. Signals d and y are related by

$$d = d_0 - \alpha^\intercal y \,,$$

where $\alpha^\intercal y$ corresponds to a dedicated source of disturbances, measurable up to the unknown scale factor α; and $\alpha \in \mathbb{R}^p$ captures a physical parameter, such as the gain of an unmodeled pathway from sensor to plant. For example, in robots with joint torque sensors, $\alpha^\intercal y$ is the torque measurement, and α is the unknown torque sensor gains [10], [24]. Finally, d_0 represents a residual, fully unmeasurable disturbance component.

We consider a regulator of the form:

$$u = u_s + u_r + u_{im} \tag{3a}$$

$$u_r = -\hat{\alpha}^\intercal y \,, \tag{3b}$$

where u_s is for closed-loop stability; $u_r = -\hat{\alpha}^\intercal y$ is the feedforward control input with $\hat{\alpha}(t) \in \mathbb{R}^p$ an estimate of α; and u_{im} is a component to reject unmeasurable disturbances. To formulate a meaningful regulator problem that includes the use of feedforward control, the following requirements should be considered:

- R1) *Regulation:* the unforced closed-loop system, obtained by setting $\zeta = \zeta_i = 0$, is stable and $x \to 0$.
- R2) *Optimality:* feedforward control u_r should be prioritized over u_{im} for disturbance rejection.
- R3) *Robustness:* brief disturbances measurable through y must be rejected instantaneously.

The requirement (R1) captures the classical requirements of closed-loop stability and steady-state regulation, whereas (R2) and (R3) are additional requirements that aim to exploit the main advantages of feedforward control in disturbance rejection: low complexity, fast reaction time, and the ability to reject brief disturbances. Requirement (R2) captures the idea that because feedforward controls are of low complexity, they should be prioritized over more costly algorithms such as adaptive internal models, especially over long time horizons. Thus, a design in which (R2) is violated over a short timescale may be acceptable, as it does not induce significant degradation in the long-term cost of operation. (R3) imposes that brief disturbances measurable through y should be nearly undetectable in the system state. This requirement cannot be achieved by an adaptive internal model, which is intended to deal with persistent, not brief disturbances. The revelance of (R3) can be understood from a neuroscience example: subjects with an impaired vestibuloocular reflex (VOR) complain they cannot read signs while walking due to the impulsive disturbance on eye position from their own footfalls [30]. (R3) highlights that the common mantra in control theory that brief disturbances can be compensated through exponential stability or classical robust control methods is not adequate for high performing control systems such as neuroscience systems.

The considered disturbance rejection problem is challenging due to the difficulty of achieving (R1)–(R3) simultaneously. A design that meets (R1) by exploiting y in the most expedient way will typically fail (R3); achieving (R3) may violate (R2); and so forth. To appreciate such tradeoffs, we consider an example. Suppose A is Hurwitz (possibly after state feedback), $y = \sin(\omega t)$, $\alpha \in \mathbb{R}$, and the nominal disturbance is:

$$d(t) = d_0(t) - \alpha y(t) = a_0 \cos(\omega t) - \alpha \sin(\omega t) \,.$$

Let $u_{im} = \hat{\psi}^\intercal \hat{w}$ be the output of an adaptive internal model with a regressor $\hat{w}(t) \in \mathbb{R}^2$ that has no direct access to y, and let $u_r = -\hat{\alpha} y$ be the feedforward input. Even if disturbance rejection is achieved asymptotically; namely $u = u_r + u_{im} \to d$, we cannot expect $\hat{\alpha} \to \alpha$ because the components of the regressor $(\hat{w}, y)$ may have redundant frequency content, making the regressor non-persistently exciting. Now suppose y includes a perturbation $\delta(t)$ (e.g., see Section IV-A) such that $y(t) = \sin(\omega t) + \delta(t)$. Then in steady-state $u - d_0(t) + \alpha y(t) \simeq (\alpha - \hat{\alpha})\delta(t) \neq 0$. That is, (R3) is violated despite (R1) being satisfied. Consider instead a case when y provides a full measurement of disturbances and $u_{im} = 0$. Let the nominal disturbances be $d_0 = \sin(\omega t)$, $y = \sin(\omega t)$, and $\alpha = 1$. In this case two disturbance sources cancel each other out, resulting in a total disturbance $d = 0$. This scenario naturally causes ambiguities for adaptation of $\hat{\alpha}$. If the objective is to achieve (R1) and (R2), then we expect $\hat{\alpha} \to 0$. Then if $y(t) = \sin(\omega t) + \delta(t)$, in steady-state we find $u - d \simeq \delta(t)$ so (R3) is not satisfied. Suppose instead (R3) is the dominant requirement. Then we require $\hat{\alpha} \to 1$, whereas standard algorithms would generate $\hat{\alpha} \to 0$. In sum, the central technical problem in achieving (R1)–(R3) simultaneously is the possible redundancy in frequency content between measured and unmeasured components of the disturbance.

III. TWO TIMESCALE REGULATOR

We aim to solve a disturbance rejection problem for system (1) with partial disturbance measurement y generated by (2), with $\alpha \in \mathbb{R}^p$ a physical parameter, subject to the requirements (R1)–(R3). The design was conceived after a study of the cerebellum and its relationship to the brainstem (housing oculomotor reflexes); see Section IV-B. It consists of two parts: (i) an adaptive internal model with a stabilizer; and (ii) a reflex adaptation law. First we require some standard definitions and assumptions.

Definition 1: The signal $w(t)$ is *persistently exciting* (PE) if there exists $\beta_0,\ \beta_1,\ T > 0$ such that

$$\beta_0 I \preceq \frac{1}{T} \int_t^{t+T} w(\tau) w^\intercal(\tau)\, d\tau \preceq \beta_1 I \,, \quad \forall\, t \geq 0 \,.$$

Definition 2: The signal $r(t) \in \mathbb{R}^m$ is *sufficiently rich of order* s if s is the smallest integer such that there exists $Q \in \mathbb{R}^{m \times s}$ and $S \in \mathbb{R}^{s \times s}$, with S having simple eigenvalues

on the $j\omega$-axis, such that

$$\dot{\zeta} = S\zeta$$
$$r = Q\zeta\,.$$

If $r(t) = 0$, then it is *sufficiently rich of order 0*.

Assumption 1: The open-loop system (1) and the measurement (2) satisfy:

- A1) the pair (A, B) is known and controllable;
- A2) the matrices S and S_i for $1 \le i \le p$ only have simple eigenvalues on the $j\omega$-axis;
- A3) wlog the pairs (Γ, S) and (Γ_i, S_i) for $1 \le i \le p$ are observable;
- A4) the dimension q is interpreted as a known upper bound on the sufficient richness of d and y;
- A5) the measurements are x and y.

Remark 1: To explain why the dimensions of S and S_i being q is wlog, we note that by (A4) there always exists S and S_i whose dimensions are at most q (see Definition 2). Now if any of these matrices were of dimension less than q, then it could be augmented to the desired dimension. This would increase the dimensionality of the associated exosystem state, and so any additional components are initialized with zero initial condition to recover the desired signals (d or y_i). ◁

Remark 2: At first glance, it may appear that (A2) and (A4) are in conflict. For example, if d contains a constant bias and q is even, then S cannot be real-valued while only having simple eigenvalues on the $j\omega$-axis. This can be addressed by (i) always assuming q is odd, (ii) letting the unexcited modes of S be any stable mode, or (iii) letting S be complex-valued. Regardless, the upcoming developments are unchanged. The same remark applies to the S_i. ◁

A. ADAPTIVE INTERNAL MODEL

While in principle any internal model and stabilizer can be used, we consider a specific design borrowing from the known literature [31] to keep our developments concrete. Our unique contribution is instead the reflex adaptation law for the feedforward gain $\hat{\alpha}$, presented in the next subsection.

Define $\tilde{\alpha} := \hat{\alpha} - \alpha$ and apply the feedforward control u_r to (1). The resulting system is

$$\dot{x} = Ax + B(u_s + u_{im}) - B(d_0 + \tilde{\alpha}^\mathsf{T} y) \tag{4a}$$
$$= Ax + B(u_s + u_{im}) - Bd - B\hat{\alpha}^\mathsf{T} y\,. \tag{4b}$$

We can see from (4a) that the goal of u_{im} will be to reject the *residual disturbance* $d_0 + \tilde{\alpha}^\mathsf{T} y$. Based on the equivalence in (4b), our approach will be to build a disturbance observer for d and another one for y., Using (A2) and (A3), we can apply the exosystem parameterization in [31], which says that for any controllable pair (F, G) selected by the designer such that F is Hurwitz, there exists a parameter $\psi_0 \in \mathbb{R}^q$ such that

$$\dot{w}_0 = Fw_0 + Gd$$
$$d = \psi_0^\mathsf{T} w_0\,.$$

Notice that ψ_0 captures all relevant unknown information about the exosystem. We use the minimal order observer from [31] to build the disturbance observer

$$\dot{\eta} = F\eta + (FN - NA)x - NBu \tag{5a}$$
$$\hat{w}_0 = \eta + Nx\,, \tag{5b}$$

where $N \in \mathbb{R}^{q\times n}$ is selected so that $NB = -G$. Next we build the internal model for y. Again applying the exosystem parameterization of [31], one obtains

$$\dot{w}_i = Fw_i + Gy_i$$
$$y_i = \psi_i^\mathsf{T} w_i$$

for some $\psi_i \in \mathbb{R}^q$. We then construct the disturbance observers

$$\dot{\hat{w}}_i = F\hat{w}_i + Gy_i\,. \tag{6}$$

Remark 3: The filters (6) can be constructed each with their own pair (F_i, G_i) provided the pair is controllable and F_i is Hurwitz. We selected $(F, G) = (F_i, G_i)$ for all i to keep the design as simple as possible. ◁

Overall, the disturbance u_{im} must reject is

$$d_0 + \tilde{\alpha}^\mathsf{T} y = d + \hat{\alpha}^\mathsf{T} y = \psi^\mathsf{T}(\hat{\alpha})w$$
$$:= \begin{bmatrix}\psi_0^\mathsf{T} & \hat{\alpha}^\mathsf{T}\end{bmatrix}\begin{bmatrix} I & 0 & 0 & 0 \\ 0 & \psi_1^\mathsf{T} & 0 & 0 \\ 0 & 0 & \ddots & 0 \\ 0 & 0 & 0 & \psi_p^\mathsf{T}\end{bmatrix}\begin{bmatrix} w_0 \\ w_1 \\ \vdots \\ w_p\end{bmatrix},$$

where $w(t) := (w_0, \ldots, w_p)(t) \in \mathbb{R}^{q(p+1)}$. Defining the estimation error $\tilde{w} := \hat{w} - w$ where $\hat{w} := (\hat{w}_0, \ldots, \hat{w}_p)$ is constructed using the observers (5)–(6), the closed-loop system becomes

$$\dot{x} = Ax + B(u_s + u_{im}) - B\psi^\mathsf{T}(\hat{\alpha})w$$
$$\dot{\tilde{w}} = \mathrm{diag}(F)\tilde{w}\,.$$

As the above system is in a standard form, the regulator design to achieve (R1) is straightforward. Let $K \in \mathbb{R}^n$ be such that $A_{cl} := A + BK^\mathsf{T}$ is Hurwitz and let $P \succ 0$ solve the Lyapunov equation $A_{cl}^\mathsf{T} P + PA_{cl} = -I$. Using the observers (5)–(6), the controller is

$$u_s = K^\mathsf{T} x \tag{7a}$$
$$u_{im} = \hat{\psi}^\mathsf{T}\hat{w} \tag{7b}$$
$$\dot{\hat{\psi}} = -\gamma(B^\mathsf{T} Px)\hat{w}\,, \tag{7c}$$

where $\gamma > 0$ and $\hat{\psi}(t) \in \mathbb{R}^{q(p+1)}$ is an estimate of the time-varying $\psi(\hat{\alpha}(t))$.

Remark 4: As mentioned after (4), a design decision was taken to construct separate disturbance observers for d and for y. A consequence of this choice is that the disturbance observer (5) for d requires the measurement y as an input through u_r. We call this variant a *centralized design* because

(possibly remote) sensory measurements y must be communicated to a centralized adaptive internal model. The centralized design creates an overparameterization of the disturbance by using multiple observers, reminiscent of Kreisselmeier filters [32]. The benefit is a simpler reconstruction of the disturbance and subsequent simpler stability analysis, because the level of excitation in regressors of the internal model does not vanish. ◁

Remark 5: Our proposed regulator design is built up from standard assumptions developed over 50 years of study in output regulation. This collective wisdom may nevertheless leave some readers unsure if practical designs are always achieved. Here we address two key points. First, we consider a matched disturbance form of the plant (1), a starting point for many papers on output regulation. It arises after applying a coordinate transformation based on the Francis regulator equations, which guarantee that a matched form always exists [8], [23]. The physical model need not be in matched form initially. We have started our design with the matched form simply to skip those extra details.

Second, a key assumption in almost all output regulation papers for linear systems is that the disturbance can be modeled by a linear exosystem, despite the fact that, in practice, disturbances contain noise, brief impulsive disturbances, and other disturbance components. The utility of the assumption is to allow a control design to proceed for a *nominal disturbance* which the designer has determined either to contain the dominant frequency components, or in the adaptive case, to be of sufficiently high order to capture the number of frequency components affecting the plant. Assuming that the closed-loop system is exponentially stable, robustness to *unmodeled disturbances* is achieved [33]. Noisy measurements, present in all practical systems, are handled by the same robustness arguments. A key theme of our article is that a significant improvement in robustness to unmodeled disturbances can be obtained by adaptive feedforward control.

In sum, any violation of regulator theory assumptions is dealt with by the robustness of the closed-loop system, yielding a bounded steady-state error due to noise in measurements, noise in the plant dynamics, or unmatched disturbances. The resulting steady-state error is small if the above effects are small. ◁

B. REFLEX ADAPTATION LAW

The key idea underlying the reflex adaptation law is the following. If $\hat{\alpha}$ is adapted very slowly or is constant, then the internal model principle will be satisfied if $u_{im} \to d_0 + \tilde{\alpha}^\intercal y$ in steady-state, by (4a). This observation justifies an interpretation of u_{im} as a metric of the quality of the feedforward control: the less well adapted the gains $\hat{\alpha}$ are, the more work must be performed by the internal model to suppress disturbances. We want to reduce this work by prioritizing feedforward control vis-à-vis (R2). Accordingly, we define a cost function

$$J_{im} := \frac{1}{2} u_{im}^2 ,$$

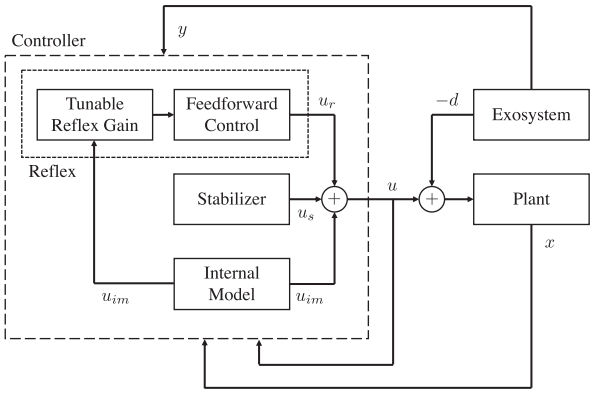

FIGURE 1. Block diagram of the two timescale regulator design.

where $u_{im} = d_0 + \tilde{\alpha}^\intercal y$ in steady-state. The resulting gradient law for reflex adaptation is

$$\dot{\hat{\alpha}} = -\varepsilon(\partial_{\hat{\alpha}} J_{im})^\intercal = -\varepsilon u_{im} y , \tag{8}$$

where $\varepsilon > 0$ will be selected sufficiently small to induce a separation of timescales. A block diagram of the overall regulator is given in Fig. 1.

Remark 6: Several design decisions have been incorporated to address (R2)–(R3). First, we can see that the cost J_{im} on the output of the internal model is intended to capture the idea that the work of the internal model must be reduced by the feedforward control. The resulting gradient adaptation law for $\hat{\alpha}$ then offloads that work, thus prioritizing the action of the feedforward control as per (R2). To achieve (R3) several issues come to play. First, there is the requirement that $\hat{\alpha}$ should converge to the constant value α. To this end, the adaptation law (8) is run slowly to allow u_{im} to achieve steady-state so that it is useful as an error signal for a reflex adaptation law that should drive $\tilde{\alpha} \to 0$. Slowness of the design has the added benefit of averaging out noise in y, which is always present in sensory measurements.

Second, the measurement y is not permitted to appear directly in u_{im}, and y is filtered using (6). Ideally, from the point of view of the internal model, brief disturbances are immediately vanquished by u_r; the internal model only processes the persistent aspect of disturbances (sinusoidal content, etc). The reason is that only u_r has the correct reflex gains to properly cancel this class of disturbances. Allowing the internal model to contribute to the cancellation of brief impulsive disturbances would upset the careful balance of response achieved by the feedforward controller. ◁

C. STABILITY ANALYSIS

The stability analysis involves identification of nominal fast and slow subsystems, to which averaging will be applied. The averaging analysis is carried out using Lemma 1 which provides an appealing Lyapunov characterization, placing the analysis in familiar terms. The results unfold in three steps, with increasing tightness on the bounds for regulation.

Define the parameter estimation error $\tilde{\psi} := \hat{\psi} - \psi(\hat{\alpha})$ and recall $\tilde{\alpha} := \hat{\alpha} - \alpha$. We observe that

$$\begin{aligned} u_{im} &= \psi(\hat{\alpha})^\mathsf{T} w + \tilde{\psi}^\mathsf{T} w + (\psi(\hat{\alpha}) + \tilde{\psi})^\mathsf{T} \tilde{w} \\ &= d_0 + \tilde{\alpha}^\mathsf{T} y + \tilde{\psi}^\mathsf{T} w + (\psi(\hat{\alpha}) + \tilde{\psi})^\mathsf{T} \tilde{w} \end{aligned}$$

and $\dot{\psi}(\hat{\alpha}) = \Psi \dot{\hat{\alpha}}$, where $\Psi := (0, \operatorname{diag}(\psi_i)) \in \mathbb{R}^{q(p+1)\times p}$. The resulting closed-loop system is

$$\dot{x} = A_{cl} x + B\tilde{\psi}^\mathsf{T} w(t) + B(\psi(\hat{\alpha}) + \tilde{\psi})^\mathsf{T} \tilde{w} \tag{9a}$$

$$\begin{aligned} \dot{\tilde{\psi}} = & -\gamma(B^\mathsf{T} P x) w(t) + \varepsilon \Psi y(t)(w^\mathsf{T}(t)\tilde{\psi} + y^\mathsf{T}(t)\tilde{\alpha}) \\ & + \varepsilon \Psi y(t) d_0(t) + \varepsilon \Psi y(t)(\psi(\hat{\alpha}) + \tilde{\psi})^\mathsf{T} \tilde{w} - \gamma(B^\mathsf{T} P x)\tilde{w} \end{aligned} \tag{9b}$$

$$\begin{aligned} \dot{\tilde{\alpha}} = & -\varepsilon y(t) y^\mathsf{T}(t)\tilde{\alpha} - \varepsilon y(t) w^\mathsf{T}(t)\tilde{\psi} - \varepsilon y(t) d_0(t) \\ & - \varepsilon y(t)(\psi(\hat{\alpha}) + \tilde{\psi})^\mathsf{T} \tilde{w} \end{aligned} \tag{9c}$$

$$\dot{\tilde{w}} = \operatorname{diag}(F)\tilde{w} \,. \tag{9d}$$

The time dependence t is used to emphasize that some signals are exogenous. We now proceed to analyze stability. For the sake of exposition, we introduce the following simplifying assumptions; these can be removed at the cost of additional technical developments such as perturbed stability analyses and PE decompositions [34].

Assumption 2: The system (9) satisfies:

A6) $\tilde{w} = 0$;

A7) $w(t)$ and $y(t)$ are each PE.

The PE assumption in (A7) is ubiquitous in adaptive control to be able to prove convergence of parameters [35]. In practice, regressors will generally not be PE, and a number of *modifications* of parameter adaptation laws are available to resolve the problem [36]; we recently developed a method based on biologically plausible principles in [34]. Notice that (A7) does not imply that the composite regressor $(w, y)(t)$ is PE.

Using (A6), the system (9) simplifies to

$$\begin{aligned} \begin{bmatrix} \dot{x} \\ \dot{\tilde{\psi}} \end{bmatrix} = & \begin{bmatrix} A_{cl} & Bw^\mathsf{T}(t) \\ -\gamma w(t) B^\mathsf{T} P & 0 \end{bmatrix} \begin{bmatrix} x \\ \tilde{\psi} \end{bmatrix} \\ & + \varepsilon G_f(t) \begin{bmatrix} \tilde{\psi} \\ \tilde{\alpha} \end{bmatrix} + \varepsilon \begin{bmatrix} 0 \\ \Psi y(t) d_0(t) \end{bmatrix} \end{aligned} \tag{10a}$$

$$\dot{\tilde{\alpha}} = -\varepsilon y(t) y^\mathsf{T}(t)\tilde{\alpha} + \varepsilon G_s(t)\tilde{\psi} - \varepsilon y(t) d_0(t) \tag{10b}$$

where

$$G_f(t) \begin{bmatrix} \tilde{\psi} \\ \tilde{\alpha} \end{bmatrix} = \begin{bmatrix} 0 \\ \Psi y(t) \end{bmatrix} \begin{bmatrix} w^\mathsf{T}(t) & y^\mathsf{T}(t) \end{bmatrix} \begin{bmatrix} \tilde{\psi} \\ \tilde{\alpha} \end{bmatrix},$$

and $G_s(t) = -y(t) w^\mathsf{T}(t)$ are bounded functions. The next result provides a Lyapunov function useful for two timescale averaging.

Lemma 1: Let $y(t) \in \mathbb{R}^p$ be a bounded PE regressor and suppose that its autocovariance matrix

$$R_y(0) = \lim_{T\to\infty} \frac{1}{T} \int_t^{t+T} y(\tau) y^\mathsf{T}(\tau)\, d\tau$$

exists with convergence uniform in $t \geq 0$. Consider the system

$$\dot{\tilde{\alpha}} = -\varepsilon y(t) y^\mathsf{T}(t)\tilde{\alpha} =: \varepsilon f_s(t, \tilde{\alpha}) \,.$$

There exists a converse Lyapunov function $V_s(t, \tilde{\alpha}; \varepsilon)$ and an $\varepsilon_\star > 0$ such that for all $\varepsilon \in (0, \varepsilon_\star)$, $V_s(\cdot)$ satisfies

$$b_1 \|\tilde{\alpha}\|^2 \leq V_s(t, \tilde{\alpha}; \varepsilon) \leq b_2 \|\tilde{\alpha}\|^2 \tag{11a}$$

$$\partial_t V_s(t, \tilde{\alpha}; \varepsilon) + \partial_{\tilde{\alpha}} V_s(t, \tilde{\alpha}; \varepsilon) \varepsilon f_s(t, \tilde{\alpha}) \leq -\varepsilon b_3 \|\tilde{\alpha}\|^2 \tag{11b}$$

$$\|\partial_{\tilde{\alpha}} V_s(t, \tilde{\alpha}; \varepsilon)\| \leq b_4 \|\tilde{\alpha}\| \tag{11c}$$

for some constants $b_i > 0$ independent of ε.

Proof: Following the averaging procedure from [37] or [35], define the near-identity transformation

$$U(t, \varepsilon) := I - \varepsilon \int_{t_0}^t (y(\tau) y^\mathsf{T}(\tau) - R_y(0)) \mathrm{e}^{-\varepsilon(t-\tau)}\, d\tau \,,$$

where $t_0 \geq 0$ denotes the initial time and $U(t, \varepsilon) \in \mathbb{R}^{q\times q}$. Defining a new state $\tilde{\alpha}_\circ \in \mathbb{R}^p$ as $\tilde{\alpha} = U(t, \varepsilon)\tilde{\alpha}_\circ$ and following the proof of [35, Lemma 4.2.3], one can show that there exists $\varepsilon_1 > 0$ such that for all $\varepsilon \in (0, \varepsilon_1)$ the resulting dynamics are

$$\dot{\tilde{\alpha}}_\circ = -\varepsilon R_y(0)\tilde{\alpha}_\circ + \varepsilon F(t, \tilde{\alpha}_\circ, \varepsilon) \,,$$

with $\|F(t, \tilde{\alpha}_\circ, \varepsilon)\| \leq \delta_1(\varepsilon)\|\tilde{\alpha}_\circ\|$ for some $\delta_1(\cdot) \in \mathcal{K}$ (a class-$\mathcal{K}$ function). Since $y(t)$ is PE and its autocovariance matrix exists, by [35, Proposition 2.7.1] $R_y(0) \succ 0$. Consequently we may define the Lyapunov function

$$V_{av}(\tilde{\alpha}_\circ) := \frac{1}{2} \tilde{\alpha}_\circ^\mathsf{T} R_y(0)^{-1} \tilde{\alpha}_\circ \,,$$

for which there exists $\varepsilon_2 > 0$ no larger than ε_1 such that for all $\varepsilon \in (0, \varepsilon_2)$ we have

$$\begin{aligned} & a_1 \|\tilde{\alpha}_\circ\|^2 \leq V_{av}(\tilde{\alpha}_\circ) \leq a_2 \|\tilde{\alpha}_\circ\|^2 \\ & \|\partial_{\tilde{\alpha}_\circ} V_{av}(\tilde{\alpha}_\circ)\| \leq a_4 \|\tilde{\alpha}_\circ\| \\ & \partial_{\tilde{\alpha}_\circ} V_{av}(\tilde{\alpha}_\circ)\dot{\tilde{\alpha}}_\circ \leq -\varepsilon (1 - a_4 \delta_1(\varepsilon)) \|\tilde{\alpha}_\circ\|^2 \leq -\varepsilon a_3 \|\tilde{\alpha}_\circ\|^2 \,, \end{aligned}$$

where the constants $a_i > 0$ are independent of ε. Also, following the proof of [35, Lemma 4.2.2], there exists $\delta_2(\cdot) \in \mathcal{K}$ such that

$$\|\varepsilon \int_{t_0}^t (y(\tau) y^\mathsf{T}(\tau) - R_y(0)) \mathrm{e}^{-\varepsilon(t-t_0)}\, d\tau\| \leq \delta_2(\varepsilon) \,.$$

Using the triangle inequality and reverse triangle inequality on $\tilde{\alpha} = U(t, \varepsilon)\tilde{\alpha}_\circ$, one may obtain the inequality

$$(1 - \delta_2(\varepsilon))\|\tilde{\alpha}_\circ\| \leq \|\tilde{\alpha}\| \leq (1 + \delta_2(\varepsilon))\|\tilde{\alpha}_\circ\| \,.$$

Since $U(t, \varepsilon)$ is a square matrix, to establish it is invertible it suffices to show that $\tilde{\alpha} = 0$ if and only if $\tilde{\alpha}_\circ = 0$. By the inequality above, if we pick $\varepsilon_\star > 0$ no larger than ε_2 such that for all $\varepsilon \in (0, \varepsilon_\star)$ we have $0 < a_5 \leq 1 - \delta_2(\varepsilon) \leq 1 + \delta_2(\varepsilon) \leq a_6$ for some constants $a_5, a_6 > 0$ that are independent of ε, then clearly $\tilde{\alpha} = 0$ if and only if $\tilde{\alpha}_\circ = 0$. At last, define the Lyapunov function

$$V_s(t, \tilde{\alpha}; \varepsilon) := V_{av}(U(t, \varepsilon)^{-1}\tilde{\alpha}) = V_{av}(\tilde{\alpha}_\circ) \,.$$

Leveraging our inequalities above, the quadratic bounds can be derived as

$$\begin{aligned} V_s(t,\tilde{\alpha};\varepsilon) = V_{av}(\tilde{\alpha}_\circ) &\geq a_1\|\tilde{\alpha}_\circ\|^2 \geq a_1(1+\delta_2(\varepsilon))^{-2}\|\tilde{\alpha}\|^2 \\ &\geq a_1 a_6^{-2}\|\tilde{\alpha}\|^2 =: b_1\|\tilde{\alpha}\|^2 \\ V_s(t,\tilde{\alpha};\varepsilon) = V_{av}(\tilde{\alpha}_\circ) &\leq a_2\|\tilde{\alpha}_\circ\|^2 \leq a_2(1-\delta_2(\varepsilon))^{-2}\|\tilde{\alpha}\|^2 \\ &\leq a_2 a_5^{-2}\|\tilde{\alpha}\|^2 =: b_2\|\tilde{\alpha}\|^2 \end{aligned}$$

whereas the Lie derivative bound is computed as

$$\begin{aligned} \partial_t V_s(t,\tilde{\alpha};\varepsilon) + \partial_{\tilde{\alpha}} V_s(t,\tilde{\alpha};\varepsilon)\dot{\tilde{\alpha}} &= \partial_{\tilde{\alpha}_\circ} V_{av}(\tilde{\alpha}_\circ)\dot{\tilde{\alpha}}_\circ \\ &\leq -\varepsilon a_3\|\tilde{\alpha}_\circ\|^2 \leq -\varepsilon a_3(1+\delta_2(\varepsilon))^{-2}\|\tilde{\alpha}\|^2 \\ &\leq -\varepsilon a_3 a_6^{-2}\|\tilde{\alpha}\|^2 =: -\varepsilon b_3\|\tilde{\alpha}\|^2 . \end{aligned}$$

For the partial derivative bound, note that we have

$$\begin{aligned} \|U(t,\varepsilon)^{-1}\| := \sup_{\tilde{\alpha}\neq 0}\left\{\frac{\|U(t,\varepsilon)^{-1}\tilde{\alpha}\|}{\|\tilde{\alpha}\|}\right\} &= \sup_{\tilde{\alpha}\neq 0}\left\{\frac{\|\tilde{\alpha}_\circ\|}{\|\tilde{\alpha}\|}\right\} \\ &\leq (1-\delta_2(\varepsilon))^{-1} \end{aligned}$$

so that

$$\begin{aligned} \|\partial_{\tilde{\alpha}} V_s(t,\tilde{\alpha};\varepsilon)\| &= \|\partial_{\tilde{\alpha}_\circ} V_{av}(\tilde{\alpha}_\circ)\partial_{\tilde{\alpha}}\tilde{\alpha}_\circ\| \\ &\leq a_4\|\tilde{\alpha}_\circ\|\|U(t,\varepsilon)^{-1}\| \\ &\leq a_4(1-\delta_2(\varepsilon))^{-2}\|\tilde{\alpha}\| \\ &\leq a_4 a_5^{-2}\|\tilde{\alpha}\| =: b_4\|\tilde{\alpha}\| . \end{aligned}$$

Noting that these bounds hold for all $\varepsilon \in (0,\varepsilon_\star)$ and that the constants $b_i > 0$ are independent of ε, this concludes the proof. □

Next we require a technical result on ultimate boundedness for a particular scalar ODE. This result is needed to characterize steady-state errors in Lemma 3 and Theorems 1–2.

Lemma 2: Consider the scalar system $\dot{z} = -az + r(t)$ where $a > 0$. Then $\limsup_{t\to\infty}|z(t)| \leq a^{-1}\limsup_{t\to\infty}|r(t)|$.

Proof: Let $r_\star := \limsup_{t\to\infty} r(t)$. It is wlog to assume $r_\star < \infty$, because otherwise the result is trivial. By definition, for every $\epsilon > 0$ there exists a time $t_\star \geq t_0$ such that $|r(t)| \leq r_\star + \epsilon$ for all $t \geq t_\star$. By linear time-invariance, the time solution is

$$z(t) = \mathrm{e}^{-a(t-t_\star)}z(t_\star) + \int_{t_\star}^{t}\mathrm{e}^{-a(t-\tau)}r(\tau)\,d\tau .$$

Consequently, we have

$$\begin{aligned} \limsup_{t\to\infty}|z(t)| &\leq \limsup_{t\to\infty}\int_{t_\star}^{t}\mathrm{e}^{-a(t-\tau)}(r_\star+\epsilon)\,d\tau \\ &= a^{-1}(r_\star+\epsilon) . \end{aligned}$$

Since the above inequality holds for all $\epsilon > 0$, it must hold for $\epsilon = 0$, thus concluding the proof. □

We now proceed to establishing steady-state error bounds iteratively. That is, we first establish a constant bound on the steady-state error for all states in Lemma 3. This bound is refined for the fast states $(x,\hat{\psi})$ only in Theorem 1. Then, we obtain a similar tighter bound for the slow states in Theorem 2, under an additional assumption. We will use big-$\mathcal{O}$ notation to describe these bounds.

Definition 3: For functions $f(\cdot)$ and $\delta_\circ(\cdot)$, we say $f(\varepsilon) = \mathcal{O}(\delta_\circ(\varepsilon))$ for all $\varepsilon > 0$ sufficiently small if there exists $\varepsilon_\star$, $c_\circ > 0$ such that $\|f(\varepsilon)\| \leq c_\circ\delta_\circ(\varepsilon)$ for all $\varepsilon \in (0,\varepsilon_\star)$.

The next result establishes a uniform bound on all states for all $\varepsilon > 0$ sufficiently small.

Lemma 3: Consider the system (1) and measurement (2) satisfying Assumption 1 with the regulator (3), (5)–(8). Let (10) be the closed-loop system resulting from Assumption 2. Then for all $\varepsilon > 0$ sufficiently small

$$\limsup_{t\to\infty}\|(x,\tilde{\psi},\tilde{\alpha})(t)\| = \mathcal{O}(1) .$$

Moreover, the closed-loop system is input-to-state stable (ISS) with respect to input $y(t)d_0(t)$.

Proof: By (A2) and (A7), [35, Th. 2.6.5] tells us that the equilibrium $(x,\tilde{\psi}) = (0,0)$ of

$$\begin{bmatrix}\dot{x}\\ \dot{\tilde{\psi}}\end{bmatrix} = \begin{bmatrix}A_{cl} & Bw^\intercal(t)\\ -\gamma w(t)B^\intercal P & 0\end{bmatrix}\begin{bmatrix}x\\ \tilde{\psi}\end{bmatrix} =: f_f(t,x,\tilde{\psi})$$

is globally exponentially stable (GES). Then [33, Th. 4.14] states that there exists a converse Lyapunov function $V_f(\cdot)$ satisfying

$$a_1\|(x,\tilde{\psi})\|^2 \leq V_f(t,x,\tilde{\psi}) \leq a_2\|(x,\tilde{\psi})\|^2 \tag{12a}$$

$$(\partial_t V_f + \partial_{(x,\tilde{\psi})}V_f\, f_f)(t,x,\tilde{\psi}) \leq -a_3\|(x,\tilde{\psi})\|^2 \tag{12b}$$

$$\|\partial_{(x,\tilde{\psi})}V_f(t,x,\tilde{\psi})\| \leq a_4\|(x,\tilde{\psi})\| \tag{12c}$$

Additionally, since $y(t)$ is the output of an LTI exosystem, its autocovariance matrix $R_y(0)$ exists with convergence uniform in $t \geq 0$ by [37, Appendix, Th. 6]. In conjunction with (A7), we have that the converse Lyapunov function $V_s(\cdot)$ from Lemma 1 exists for $\varepsilon > 0$ sufficiently small. With the appropriate converse Lyapunov functions now constructed, we move on to establishing the steady-state error bound.

To keep our developments concise, we will skip most of the algebra involved in the upcoming Lyapunov arguments. To aid the reader, the following facts from Young's Inequality are used:

$$\begin{aligned} \varepsilon\|(x,\tilde{\psi})\|\|\tilde{\alpha}\| &\leq \frac{1}{2}\varepsilon^{2/3}\|(x,\tilde{\psi})\|^2 + \frac{1}{2}\varepsilon^{4/3}\|\tilde{\alpha}\|^2 \\ \|\tilde{\alpha}\|\|y(t)d_0(t)\|_{\mathcal{L}_\infty} &\leq \frac{1}{2}c\|\tilde{\alpha}\|^2 + \frac{1}{2}c^{-1}\|y(t)d_0(t)\|_{\mathcal{L}_\infty}^2 \\ \|(x,\tilde{\psi})\|\|\Psi\|\|y(t)d_0(t)\|_{\mathcal{L}_\infty} &\leq \frac{1}{2}\|(x,\tilde{\psi})\|^2 + \frac{1}{2}\|\Psi\|^2\|y(t)d_0(t)\|_{\mathcal{L}_\infty}^2 , \end{aligned}$$

where $c > 0$ is an arbitrary constant, and we define the supremum norm as $\|\cdot\|_{\mathcal{L}_\infty} := \sup_{t\geq t_0\geq 0}\|\cdot\|$. Now consider the Lyapunov function $V(t,x,\tilde{\psi},\tilde{\alpha};\varepsilon) := V_f(t,x,\tilde{\psi}) + V_s(t,\tilde{\alpha};\varepsilon)$, computing its Lie derivative with respect to (10)

and applying the facts above, one obtains

$$\begin{aligned}\dot{V}(t,x,\tilde{\psi},\tilde{\alpha};\varepsilon)&\\ \leq -\left(a_3-\varepsilon^{2/3}\gamma_0-\varepsilon a_4\|G_f(t)\|_{\mathcal{L}_\infty}-\frac{1}{2}\varepsilon a_4\right)\|(x,\tilde{\psi})\|^2&\\ -\varepsilon\left(b_3-\frac{1}{2}b_4c-\varepsilon^{1/3}\gamma_0\right)\|\tilde{\alpha}\|^2&\\ +\frac{1}{2}\varepsilon\left(a_4\|\Psi\|^2+b_4c^{-1}\right)\|y(t)d_0(t)\|^2_{\mathcal{L}_\infty},&\end{aligned}$$

where $\gamma_0 := \frac{1}{2}(a_4\|G_f(t)\|_{\mathcal{L}_\infty}+b_4\|G_s(t)\|_{\mathcal{L}_\infty})$. Since $c>0$ is arbitrary, we may select it independently of ε so that $b_3-\frac{1}{2}b_4c>0$. Then it is clear that for all $\varepsilon>0$ sufficiently small, we have (omitting details)

$$\dot{V}(\cdot)\leq-\gamma_1\|(x,\tilde{\psi})\|^2-\varepsilon\gamma_2\|\tilde{\alpha}\|^2+\varepsilon\gamma_3\|y(t)d_0(t)\|^2_{\mathcal{L}_\infty}$$

for some $\gamma_1,\ \gamma_2,\ \gamma_3>0$ independent of ε. Since we are restricting our attention to $\varepsilon>0$ sufficiently small, and because $V_f(\cdot)$ and $V_s(\cdot)$ are upper bounded by quadratics in their states, it is wlog to state that there exists $\gamma_\star>0$ independent of ε such that

$$\dot{V}(\cdot)\leq-\varepsilon\gamma_\star V(\cdot)+\varepsilon\gamma_3\|y(t)d_0(t)\|^2_{\mathcal{L}_\infty}. \tag{13}$$

As such, one immediately concludes ISS with respect to $y(t)d_0(t)$ [33, Th. 4.19]. Using the Comparison Lemma and Lemma 2, one deduces

$$\limsup_{t\to\infty}V(t,x(t),\tilde{\psi}(t),\tilde{\alpha}(t);\varepsilon)\leq\gamma_3\gamma_\star^{-1}\|y(t)d_0(t)\|^2_{\mathcal{L}_\infty},$$

where $\gamma_3\gamma_\star^{-1}\|y(t)d_0(t)\|^2_{\mathcal{L}_\infty}=\mathcal{O}(1)$. Given that $V(\cdot)$ is lower bounded by a quadratic in $(x,\tilde{\psi},\tilde{\alpha})$, the above expression proves the result. □

The first stability result addresses regulation of $(x,\hat{\psi})$.

Theorem 1: Consider the system (1) and measurement (2) satisfying Assumption 1 with the regulator (3), (5)–(8). Let (10) be the closed-loop system resulting from Assumption 2. Then for all $\varepsilon>0$ sufficiently small

$$\limsup_{t\to\infty}\|(x,\tilde{\psi})(t)\|=\mathcal{O}(\varepsilon).$$

Proof: Taking the Lie derivative of $V_f(\cdot)$ from (12) with respect to (10a), we have

$$\begin{aligned}\dot{V}_f(t,x,\tilde{\psi})&\leq-a_3\|(x,\tilde{\psi})\|^2+a_4\|(x,\tilde{\psi})\|\varepsilon r(t)\\ &\leq-\left(a_3-\frac{1}{2}a_4c\right)a_1^{-1}V_f(t,x,\tilde{\psi})\\ &\quad+\frac{1}{2}\varepsilon^2a_4c^{-1}r^2(t),\end{aligned}$$

where $r(t):=\|G_f(t)\|_{\mathcal{L}_\infty}\|(\tilde{\psi},\tilde{\alpha})(t)\|+\|\Psi\|\|y(t)d_0(t)\|_{\mathcal{L}_\infty}$ and $c>0$ independent of ε is selected so that $a_3-\frac{1}{2}a_4c>0$. Note that the second inequality is obtained through an appropriate application of Young's Inequality. Using the Comparison Lemma and Lemma 2, we obtain

$$\limsup_{t\to\infty}V_f(t,x(t),\tilde{\psi}(t))\leq\varepsilon^2\gamma_\star\left(\limsup_{t\to\infty}r^2(t)\right)$$

for some $\gamma_\star>0$ sufficiently large and independent of ε. By Lemma 3 we have that for all $\varepsilon>0$ sufficiently small

$$\begin{aligned}\limsup_{t\to\infty}r(t)&=\|G_f(t)\|_{\mathcal{L}_\infty}\left(\limsup_{t\to\infty}\|(\tilde{\psi},\tilde{\alpha})(t)\|\right)\\ &\quad+\|\Psi\|\|y(t)d_0(t)\|_{\mathcal{L}_\infty}=\mathcal{O}(1).\end{aligned}$$

Using the fact $r(t)\geq0$, we have $\limsup_{t\to\infty}r^2(t)=(\limsup_{t\to\infty}r(t))^2$ and so we conclude

$$\limsup_{t\to\infty}V_f(t,x(t),\tilde{\psi}(t))=\mathcal{O}(\varepsilon^2)$$

for all $\varepsilon>0$ sufficiently small. Lastly, the lower bound $a_1\|(x,\tilde{\psi})\|^2\leq V_f(t,x,\tilde{\psi})$ proves the result. □

Theorem 1 shows that regulation of $(x,\tilde{\psi})$ can be achieved up to order ε. Since (R1) is generally the overriding control objective, this result confirms that our two timescale design provides a practical solution to the disturbance rejection problem, while also achieving (R2). However, the previous result draws no conclusions about the convergence of the slow state $\hat{\alpha}$, implying that we do not know if the design can also achieve (R3). The next stability result gives a sufficient condition for regulation of $\hat{\alpha}$.

Theorem 2: Consider the system (1) and measurement (2) satisfying Assumption 1 with the regulator (3), (5)–(8). Let (10) be the closed-loop system resulting from Assumption 2. Additionally, suppose that $y(t)d_0(t)$ has zero average. Then for all $\varepsilon>0$ sufficiently small

$$\limsup_{t\to\infty}\|\tilde{\alpha}(t)\|=\mathcal{O}(\varepsilon).$$

Proof: By linearity we may split (10b) as

$$\begin{aligned}\dot{\tilde{\alpha}}_1&=-\varepsilon y(t)y^{\mathsf{T}}(t)\tilde{\alpha}_1+\varepsilon G_s(t)\tilde{\psi}(t)\\ \dot{\tilde{\alpha}}_2&=-\varepsilon y(t)y^{\mathsf{T}}(t)\tilde{\alpha}_2-\varepsilon y(t)d_0(t),\end{aligned}$$

where $\tilde{\alpha}=\tilde{\alpha}_1+\tilde{\alpha}_2$, with $\tilde{\alpha}_1(t),\ \tilde{\alpha}_2(t)\in\mathbb{R}^p$, and $\tilde{\alpha}_2(t_0)=0$. By the same reasoning presented in the proof of Lemma 3, we have that $V_s(\cdot)$ from Lemma 1 exists for all $\varepsilon>0$ sufficiently small. Taking the Lie derivative of $V_s(\cdot)$ along the $\tilde{\alpha}_1$ dynamics we obtain

$$\begin{aligned}\dot{V}_s(t,\tilde{\alpha}_1;\varepsilon)&\leq-\varepsilon b_3\|\tilde{\alpha}_1\|^2+\varepsilon b_4\|\tilde{\alpha}_1\|\|G_s(t)\|_{\mathcal{L}_\infty}\|\tilde{\psi}(t)\|\\ &\leq-\varepsilon\left(b_3-\frac{1}{2}b_4c\right)b_1^{-1}V_s(t,\tilde{\alpha}_1;\varepsilon)\\ &\quad+\frac{1}{2}\varepsilon b_4c^{-1}\|G_s(t)\|^2_{\mathcal{L}_\infty}\|\tilde{\psi}(t)\|^2,\end{aligned}$$

where $c>0$ independent of ε is selected so that $b_3-\frac{1}{2}b_4c>0$. By the Comparison Lemma and Lemma 2, followed by Theorem 1 which states $\limsup_{t\to\infty}\|\tilde{\psi}(t)\|=\mathcal{O}(\varepsilon)$, we have that there exists $\gamma_\star>0$ independent of ε such that

$$\begin{aligned}\limsup_{t\to\infty}V_s(t,\tilde{\alpha}_1(t);\varepsilon)&\leq\gamma_\star\left(\limsup_{t\to\infty}\|\tilde{\psi}(t)\|^2\right)\\ &=\gamma_\star\left(\limsup_{t\to\infty}\|\tilde{\psi}(t)\|\right)^2=\mathcal{O}(\varepsilon^2).\end{aligned}$$

Using the lower bound $V_s(t, \tilde{\alpha}_1; \varepsilon) \geq b_1 \|\tilde{\alpha}_1\|^2$, we conclude

$$\limsup_{t\to\infty} \|\tilde{\alpha}_1(t)\| = \mathcal{O}(\varepsilon)\,.$$

Next, since $y(t)d_0(t)$ is assumed to have zero average, the average dynamics of $\tilde{\alpha}_2$ are

$$\dot{\tilde{\alpha}}_{av} = -\varepsilon R_y(0)\tilde{\alpha}_{av}\,,$$

where $\tilde{\alpha}_{av}(t) \in \mathbb{R}^p$ and $\tilde{\alpha}_{av}(t_0) = \tilde{\alpha}_2(t_0) = 0$. Note that, using [37, Appendix, Th. 6], $R_y(0)$ exists with convergence uniform in $t \geq 0$ because $y(t)$ is the output of an LTI exosystem. Given that $y(t)$ is PE by (A7), we have that $R_y(0) \succ 0$ by [35, Proposition 2.7.1]. Thus $-\varepsilon R_y(0)$ is Hurwitz and so the equilibrium $\tilde{\alpha}_{av} = 0$ is GES. By the Hovering Theorem [38, Th. 5.5.1], there exists $\delta_{av}(\cdot) \in \mathcal{K}$ yielding the bound

$$\|\tilde{\alpha}_2(t)\|_{\mathcal{L}_\infty} = \|\tilde{\alpha}_2(t) - \tilde{\alpha}_{av}(t)\|_{\mathcal{L}_\infty} = \mathcal{O}(\delta_{av}(\varepsilon))$$

for all $\varepsilon > 0$ sufficiently small, where we note $\tilde{\alpha}_{av}(t) = 0$ because $\tilde{\alpha}_{av}(t_0) = 0$. In fact, we may take $\mathcal{O}(\delta_{av}(\varepsilon)) = \mathcal{O}(\varepsilon)$ by [38, Lemma 4.6.5] since $y(t)$ is a finite sum of sinusoids given that it is the output of an LTI exosystem. At last, the triangle inequality gives us that

$$\begin{aligned}\limsup_{t\to\infty} \|\tilde{\alpha}(t)\| &\leq \limsup_{t\to\infty} \|\tilde{\alpha}_1(t)\| + \|\tilde{\alpha}_2(t)\|_{\mathcal{L}_\infty} \\ &= \mathcal{O}(\varepsilon) + \mathcal{O}(\varepsilon) = \mathcal{O}(\varepsilon)\,,\end{aligned}$$

as desired. □

Remark 7: While not reiterated in Theorems 1–2, the ISS property in Lemma 3 still holds, highlighting the robustness of the proposed design. A special case of the foregoing results is that if $d_0 = 0$, meaning y provides a full measurement of the disturbance up to a scale factor, and Assumption 2 holds, then the equilibrium $(x, \tilde{\psi}, \tilde{\alpha}) = (0, 0, 0)$ is GES, implying again robustness. Surprisingly, even in this special case, our proposed two timescale design is needed to meet (R3). This will be shown in Section IV-B. More generally, if $d_0 \neq 0$ one cannot guarantee regulation of $\hat{\alpha}$ to the physical parameter α, indicative of interference between the internal model and the feedforward control. Theorem 2 tells us that this interference vanishes if the unmeasured component of the disturbance d_0 is, in an average sense, uncorrelated with the measured component y. This requirement is reasonable in many engineering applications where d_0 and y represent two different sources of environmental disturbances. ◁

An alternative interpretation of Theorem 2 is that $\hat{\alpha}$ will converge near a value of α that de-correlates the unmeasured disturbance d_0 from the measurement y. This value of α always exists and can be computed as follows.

Proposition 1: Suppose $y(t) \in \mathbb{R}^p$ is PE, its autocovariance matrix $R_y(0)$ exists, and the average of $y(t)d(t)$ exists. Define $d_0 := d + \alpha^\intercal y$. Then there exists a unique $\alpha \in \mathbb{R}^p$ such that $y(t)d_0(t)$ has zero average.

Proof: We want to find α solving the linear equation

$$\begin{aligned}0 &= \lim_{T\to\infty} \frac{1}{T}\int_t^{t+T} y(\tau)d_0(\tau)\,d\tau \\ &= \lim_{T\to\infty} \frac{1}{T}\int_t^{t+T} y(\tau)d(\tau)\,d\tau + R_y(0)\alpha\,.\end{aligned}$$

Since $y(t)$ is PE, $R_y(0)$ is invertible [35, Proposition 2.7.1] and one can directly solve for α. □

IV. EXAMPLES

This section presents two examples. The first pedagogical example compares our design to standard adaptive control designs, thus motivating why the proposed design is required to satisfy (R1)–(R3). The second example regards the VOR, where we demonstrate the biological plausibility of our model by considering standard experiments with long-term adaptation of the VOR gain.

A. THIRD-ORDER EXAMPLE

In the first example we compare our proposed regulator design with two standard regulators. Consider a third order system of the form (1) with parameters

$$A = \begin{bmatrix}0 & 1 & 0\\ 0 & 0 & 1\\ 0 & 0 & 0\end{bmatrix}, \quad B = \begin{bmatrix}0\\ 0\\ 1\end{bmatrix}, \quad x(t_0) = \begin{bmatrix}10\\ 0\\ 0\end{bmatrix}.$$

Unspecified initial conditions are zero. The nominal disturbance is $d(t) = 20\cos(2\pi t) - 20\sin(2\pi t)$. We assume a partial disturbance measurement $y(t) = \sin(2\pi t)$, so that $d = d_0 - \alpha^\intercal y$ with $\alpha = 20$ and $d_0(t) = 20\cos(2\pi t)$. The controller has the form

$$\begin{aligned}u &= u_s + u_{im} + u_r\,,\\ u_s &= K^\intercal x\,, \quad u_{im} = \hat{\psi}^\intercal \hat{w}\,, \quad u_r = -\hat{\alpha}^\intercal y\,,\end{aligned}$$

where $K^\intercal = \begin{bmatrix}-6 & -11 & -6\end{bmatrix}$ for closed-loop stability. Let $P \succ 0$ solve the Lyapunov equation $A_{cl}^\intercal P + PA_{cl} = -I$, where $A_{cl} := A + BK^\intercal$, and select

$$F = \begin{bmatrix}0 & 1\\ -1 & -1\end{bmatrix}, \quad G = \begin{bmatrix}0\\ 1\end{bmatrix}, \quad N = -GB^\intercal\,, \quad \gamma = 100\,.$$

We model brief impulsive disturbances as short square pulses of the form $\delta(t; t_*, \Delta t) = H(t - t_*) - H(t - (t_* + \Delta t))$, where $H(\cdot)$ is the Heaviside step function and $\Delta t > 0$ is selected small. The perturbed measurement and disturbance are assumed to be

$$\begin{aligned}y(t) = {}& \sin(2\pi t)\\ &+ 20\,(\delta(t; t_1, \Delta t) - \delta(t; t_2, \Delta t) + \delta(t; t_3, \Delta t))\\ d(t) = {}& 20\cos(2\pi t) - 20y(t)\,,\end{aligned}$$

with $t_1 = 20.5$, $t_2 = 40.5$, $t_3 = 60.5$, and $\Delta t = 0.1$. The convention in our Figures is that each state is plotted as a gradient of the same colour, where the darkest plot corresponds to the first component and the lightest plot corresponds to the last component.

Standard Design I: As a first baseline controller, we consider a standard regulator design that does not use the

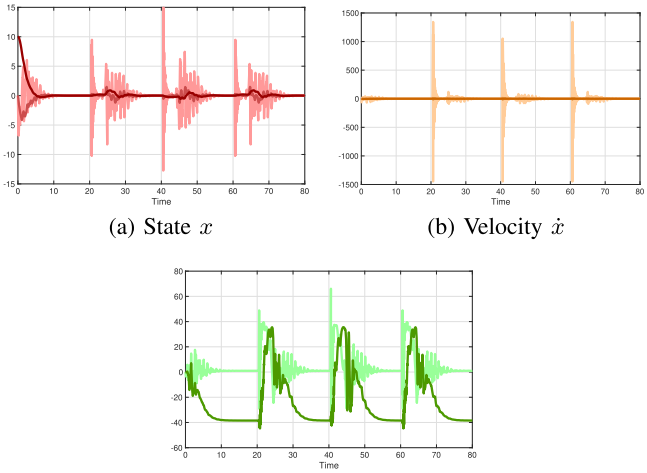

(a) State x (b) Velocity $\dot{x}$

(c) Internal Model Parameter $\hat{\psi}$

FIGURE 2. Standard regulator with no reflex.

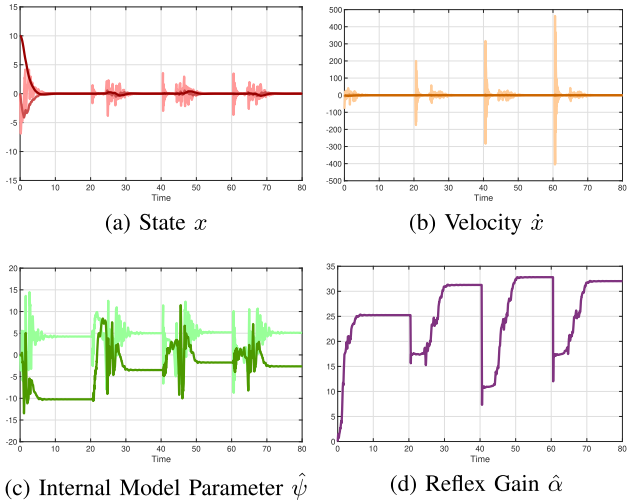

(a) State x (b) Velocity $\dot{x}$

(c) Internal Model Parameter $\hat{\psi}$ (d) Reflex Gain $\hat{\alpha}$

FIGURE 3. Standard regulator with reflex. The vertical axes for $\dot{x}$ has been reduced from ±1500 in Fig. 2 to ±500.

measurement y. It consists of the disturbance observer (5) (where $\hat{w} = \hat{w}_0$) with

$$\dot{\hat{\psi}} = -\gamma(B^\mathsf{T}Px)\hat{w}$$
$$u_r = 0\,.$$

In Fig. 2 we observe that the state x is initially regulated to zero (as desired), followed by three episodes of disturbance rejection that coincide with the brief impulsive disturbances occurring at times t_i. One sees that in each episode of disturbance rejection there are two phases: an initial response at time t_i followed by a more prolonged period of regulation in which $x \to 0$. Comparing with the settling time of the parameter $\hat{\psi}$ in Fig. 2(c), we deduce that the more prolonged phase of each episode is due to the correction of the internal model parameter and not the immediate effect of the brief impulsive disturbance. This is further supported by the consistency of this phase of the response with other regulators presented later. Fig. 2(b) also shows a plot of $\dot{x}$, which we include as a measure of the quality of disturbance rejection of brief impulsive disturbances (for the oculomotor system, small retinal slip velocity is a requirement for proper vision). Overall for this design, one observes a large deviation in x and very large spikes in $\dot{x}$ on the order of 1000 in magnitude. Clearly the robustness requirement (R3) is not met using this design.

Standard Design II: A second regulator design includes measurement y in the most expedient way, namely $u_r = -\hat{\alpha}^\mathsf{T}y$. The regressor is augmented to be $(\hat{w}, -y)$ suggesting the joint adaptation of $(\hat{\psi}, \hat{\alpha})$ using adaptation laws

$$\dot{\hat{\psi}} = -\gamma(B^\mathsf{T}Px)\hat{w}$$
$$\dot{\hat{\alpha}} = -\gamma(B^\mathsf{T}Px)(-y)\,.$$

Fig. 3 shows that the brief impulsive disturbance in the first episode is well compensated, resulting in a peak velocity around 200 (about an order of magnitude less than the first

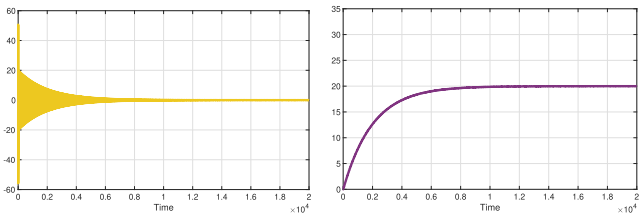

(a) Internal Model $u_{im} - d_0$ (b) Reflex Gain $\hat{\alpha}$

FIGURE 4. Nominal phase for the two timescale regulator with reflex. The time axes range in $[0, 2 \times 10^4]$ to showcase slow adaptation.

regulator design). This may be attributed to the fact that $\hat{\alpha}$ is near its true value of $\alpha = 20$ as seen in Fig. 3(d). For subsequent episodes, the peak velocity jumps up to around 500, a significant degradation in robustness. Due to the inherent lack of PE of the composite regressor $(\hat{w}, -y)$, there is no mechanism to drive $\hat{\alpha} \to \alpha$. This design shows that simply adding a feedforward controller without further thought on its effectiveness is not an acceptable design methodology.

Proposed Two Timescale Design: Finally, we consider the design of Section III, whose goal is to drive $\hat{\alpha} \to \alpha$ such that the feedforward control minimizes the work of the internal model. We set $\varepsilon = 0.001$. The simulation is preceded by a nominal disturbance rejection phase over a window $t \in [0, 2 \times 10^4]$ with $d(t) = 20\cos(2\pi t) - 20\sin(2\pi t)$ and $y(t) = \sin(2\pi t)$ to train the reflex. Fig. 4 shows that the internal model output u_{im} reduces in magnitude to d_0 while the reflex gain $\hat{\alpha}$ increases, indicating that (R2) is met. Since $y(t)d_0(t) = 20\sin(2\pi t)\cos(2\pi t)$ has zero average, then as per Theorem 2, Fig. 4(b) shows that $\hat{\alpha}$ is adapted to approximately $\alpha = 20$.

To investigate (R3), we extend the previous simulation, but now include three brief impulsive disturbances. In Fig. 5 we see the peak velocity is maintained at around 100, and that

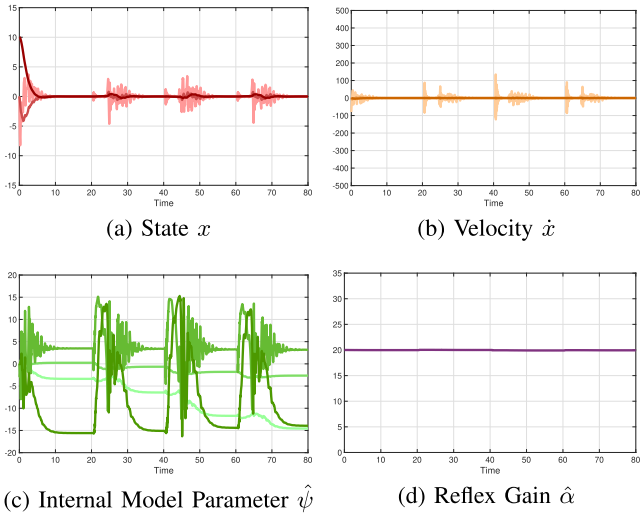

(a) State x (b) Velocity $\dot{x}$

(c) Internal Model Parameter $\hat{\psi}$ (d) Reflex Gain $\hat{\alpha}$

FIGURE 5. Two timescale regulator with reflex.

the reflex gain $\hat{\alpha}$ remains near its true value of $\alpha = 20$. Consistently superior robustness to brief impulsive disturbances is demonstrated. We conclude that (R1)–(R3) have been satisfied within reasonable tolerances. Since ε is selected small, the $\mathcal{O}(\varepsilon)$ error expected from Theorems 1–2 is hardly noticeable.

B. VESTIBULOOCULAR REFLEX

The VOR is a reflex that counteracts head movement to ensure a stable retinal image for clear vision [30]. The goal of this section is to demonstrate that our two timescale regulator design recovers the standard experiments regarding *long-term adaptation* of the *VOR gain*.

Long-term adaptation of the VOR gain was described qualitatively in the *Miles-Lisberger hypothesis* [29], which inspired our model. Consider an experiment in which a subject wears $2\times$ magnifying lenses. Horizontal head movement under abrupt magnification creates retinal slip of the visual field. Retinal slip is interpreted by the cerebellum as a sensory error signal to be driven asymptotically to zero: increased retinal slip causes increased modulation of the cerebellar output. This activity induces the *VOR gain*, a scale factor on the vestibular measurement of head velocity, to increase. An increase of VOR gain makes the VOR more effective to eliminate retinal slip during head movement, resulting in a gradual reduction in the output of the cerebellum. This adaptation of the VOR gain, which takes place over hours, results in a transfer of learning from the cerebellum to the brainstem (the site of the direct VOR pathway from ears to eyes) in a process called *consolidation* [39].

To model this process we start with a simplified model of the oculomotor plant

$$\dot{\theta} = u$$

where $\theta(t) \in \mathbb{R}$ is the horizontal eye angle in a (moving) head-fixed frame, and $u(t) \in \mathbb{R}$ is associated with the net horizontal torque on the eyeball. This model is a simplification of the second-order oculomotor plant model which includes an extra fast stable pole [40]. The first-order oculomotor plant model includes a linear drift term $A\theta$ which renders the oculomotor plant to be open-loop stable. As discussed in [27], this drift term is almost perfectly cancelled by a signal of the form $\alpha_\theta \hat{\theta}$ from the *brainstem neural integrator*, an adaptive observer that provides the estimate $\hat{\theta}$ of the horizontal eye angle. The adaptation processes associated with the brainstem neural integrator are independent of the adaptive processes modeled in this article; therefore, it has been omitted for the sake of simplicity and exposition. See the comments in Section IV-C.

The *retinal error* is the displacement of a target image on the retina from the fovea, given by

$$e := \alpha_m(r - \theta_h) - \theta$$

where $r(t) \in \mathbb{R}$ is the horizontal angular position of the target, $\theta_h(t) \in \mathbb{R}$ is the horizontal head angle, both in a world-fixed frame, and $\alpha_m(t) \in \mathbb{R}$ is a magnification factor. The goal of the oculomotor system is to drive e to zero. The VOR takes the form of an adaptive feedforward control

$$u_r = -\hat{\alpha}_h \dot{\theta}_h$$

where $\hat{\alpha}_h(t) \in \mathbb{R}$ is called the *VOR gain* and the head velocity $y := \dot{\theta}_h$ is a measurement provided by the ear's semicircular canals. It is known experimentally that $\hat{\alpha}_h$ is adapted over hours and days, while $e \to 0$ in under a few seconds.

A number of experiments can elicit slow adaptation of the VOR gain. Wearing magnifying lenses causes an abrupt change in α_m to which $\hat{\alpha}_h$ must adapt. An equivalent experiment is to make the target position a scalar multiple of the head angle; namely, $r = \alpha_r \theta_h$ [41]. The retinal error becomes

$$e = r - \theta_h - \theta = (\alpha_r - 1)\theta_h - \theta\,,$$

which corresponds to a fictitious magnification of $\alpha_m = 1 - \alpha_r$ with a reference at $r = 0$ (the brain has no direct measurement of r, so it cannot distinguish the two scenarios). Defining

$$\alpha_h := 1 - \alpha_r\,,$$

the disturbance to be rejected is $d = -\alpha_h y$. The error dynamics then become

$$\dot{e} = Ae + Bu - Bd\,, \tag{14}$$

where $A = 0$ and $B = -1$, matching the form of (1). Throughout we set $y(t) = \dot{\theta}_h(t) = 12\cos(0.2 \times 2\pi t)$, $e(t_0) = 10$, $\theta_h(t_0) = 0$, $t_0 = 0$, and we let unspecified initial conditions be zero. We select parameters $K = 5$, $\gamma = 10$, $\varepsilon = 1.5 \times 10^{-4}$, and

$$F = \begin{bmatrix} 0 & 1 \\ -1 & -1 \end{bmatrix}, \quad G = \begin{bmatrix} 0 \\ 1 \end{bmatrix}, \quad N = G\,,$$

whose values are inspired from [27], [40].

A first standard VOR experiment involves tracking a world-fixed target. This task can be emulated by setting $\alpha_r = 0$, implying that $\alpha_h = 1 - \alpha_r = 1$. Fig. 6 presents the results using our design. In Fig. 6(b) we observe that $e \to 0$ on a

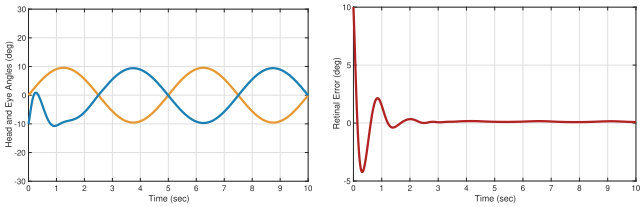

(a) θ_h (orange) and θ (blue) (b) Retinal Error e

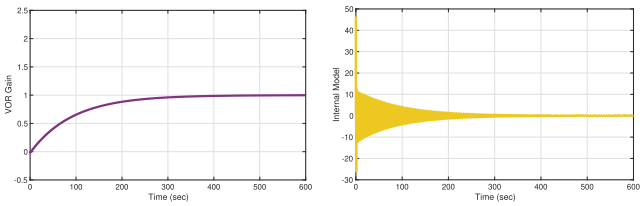

(c) VOR Gain $\hat{\alpha}_h$ (d) Internal Model u_{im}

FIGURE 6. Fast [6(a)–6(b)] and slow [6(c)–6(d)] timescale dynamics for VOR adaptation.

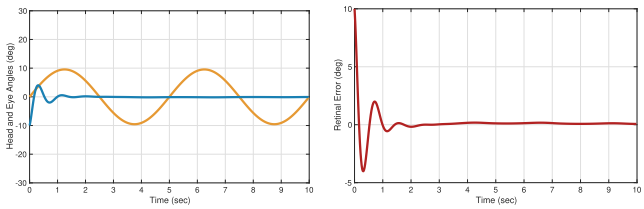

(a) θ_h (orange) and θ (blue) (b) Retinal Error e

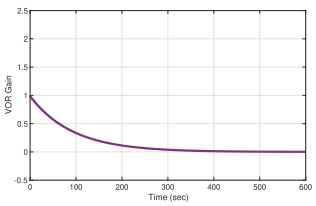

(c) VOR Gain $\hat{\alpha}_h$

FIGURE 7. Fast [7(a)–7(b)] and slow [7(c)] timescale dynamics for VOR cancellation.

fast timescale, causing the eyes to move opposite to the head with appropriate amplification. On a slow timescale, Fig. 6(c) shows that the VOR gain adapts to the steady-state value of $\alpha_h = 1$ over a few minutes, which is the condition to meet (R3). Moreover, as the VOR gain adapts we see $u_{im} \to 0$ in Fig. 6(d), clearly illustrating how a correct reflex reduces the work of the cerebellum as per (R2). Note that ε could be reduced to extend the time of long-term adaptation to hours or days rather than minutes.

A second standard experiment is called *VOR cancellation* in which a subject tracks a head-fixed target. In this case $\alpha_r = 1$ so $\alpha_h = 0$. It has been demonstrated experimentally that if VOR cancellation is sustained over a long duration, then one can attenuate the VOR gain $\hat{\alpha}_h \to 0$. Fig. 7 shows our regulator recovers this behaviour.

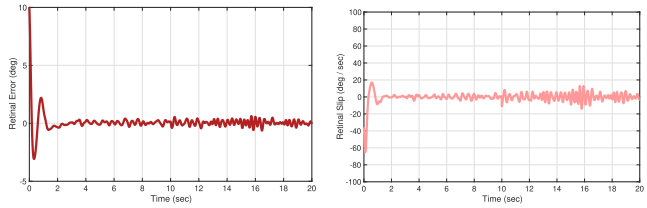

(a) Retinal Error e (b) Retinal Slip $\dot{e}$

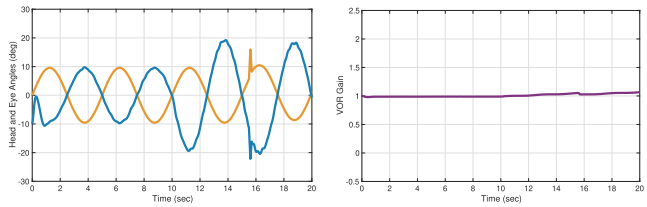

(c) θ_h (orange) and θ (blue) (d) VOR Gain $\hat{\alpha}_h$

FIGURE 8. Rejection of brief impulsive disturbances by the proposed two timescale regulator.

Finally, we investigate the extent to which our design achieves (R3) by considering a common scenario for the oculomotor system as follows. Under normal conditions, the VOR gain is adapted to its correct value near 1 over a long time horizon. Suppose the subject then puts on magnifying lenses, resulting in an instantaneous change in α_m. This change will be counteracted by the cerebellum on a short timescale (of hundreds of milliseconds) for the purpose of tracking and disturbance rejection; however, for proper oculomotor function, the brainstem VOR must still be able to cancel brief disturbances based on the physically meaningful value of $\alpha_h = 1$. To capture this scenario, we initialize the VOR gain to its nominal value of $\hat{\alpha}_h(t_0) = \alpha_h = 1$, and introduce a brief impulsive disturbance $90(\delta(t; 15.5, 0.1) - \delta(t; 15.6, 0.1))$ modelling the impact of footfalls. During $t \in [0, 10)$ we take $\alpha_r = 0$, corresponding to the standard VOR experiment described previously. Then to emulate a sudden change in α_m, we set $\alpha_r = -1$ during $t \in [10, 20)$, corresponding to a doubling of $\alpha_h = 1 - \alpha_r = 2$. Additionally, we consider a scenario where the measurements of e and y are corrupted by additive Gaussian noise having 0 mean and 0.1^2 variance. A simulation of this experiment is found in Fig. 8. It is shown that the retinal error is quickly regulated near zero, as expected. We also see that despite the short term doubling of α_h, the effect of the brief impulsive disturbance remains minimal.

To further emphasize why the proposed two timescale regulator is required to reproduce biologically plausible behaviour, consider the standard adaptive regulator design

$$\dot{\hat{\alpha}}_h = -\gamma(B^\mathsf{T} P x)(-y)$$

$$u_{im} = 0\,.$$

This simpler design (with no internal model) is a valid option as $d_0 = 0$ in our VOR examples. We simulate again the scenario of Fig. 8 using this standard design. Results are

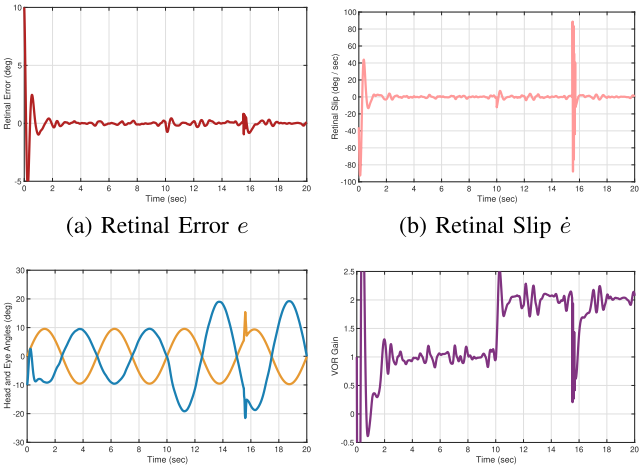

(a) Retinal Error e (b) Retinal Slip $\dot{e}$

(c) θ_h (orange) and θ (blue) (d) VOR Gain $\hat{\alpha}_h$

FIGURE 9. Rejection of brief impulsive disturbances by the standard adaptive regulator.

shown in Fig. 9, where we observe poor robustness to the brief impulsive disturbance. Considering Fig. 9(d), it is clear that fast adaptation of $\hat{\alpha}_h$ from $\hat{\alpha}_h = 1$ to $\hat{\alpha}_h = 2$ is the cause of the poor performance. From a biological standpoint, the observed behaviour is unacceptable as the large retinal slip would induce temporary blindness while walking, undermining the effectiveness of one of our key senses.

Remark 8: In practice, one may choose ε as large as 0.01 to recover qualitatively similar simulations as above. What is more important, however, is to select ε in terms of the desired precision of regulation. For example, if one desires ten times more precision in disturbance rejection, one selects ε ten times smaller, vis-à-vis our $\mathcal{O}(\varepsilon)$ error bounds. The need for precision is strongly supported by neuroscience systems which employ timescales ranging from hundreds of milliseconds to hours, if not weeks. ◁

C. BIOLOGICAL PLAUSIBILITY

The measurement structure of our model adheres to the known neural circuit associated with the slow eye movement system and the cerebellum [27], [30]. The plausibility of adaptive internal models in the cerebellum has been discussed in [27], [28]. The particular form of (5) is debatable from a neuroscience standpoint. Considering the oculomotor system, the main question is precisely what is the form of the *mossy fiber inputs* to the *flocculus*, the module of the cerebellum responsible for regulation of slow eye movements. For instance, a functionally equivalent disturbance observer to (5) resembling Kreisselmeier filters is:

$$\begin{aligned}\dot{\eta}_1 &= F\eta_1 + FNx\\ \dot{\eta}_2 &= F\eta_2 - NAx\\ \dot{\eta}_3 &= F\eta_3 - NBu\\ \hat{w}_0 &= \eta_1 + \eta_2 + \eta_3 + Nx\,.\end{aligned}$$

Here the mossy fiber inputs are individually filtered in the *granule layer* of the cerebellum using synchronized filters (with the same values of (F, N)). It is conceivable that estimates $\hat{x}$, $\hat{A}\hat{x}$, and $\hat{B}u$ of the signals x, Ax, and Bu could be provided by an adaptive observer (e.g., the brainstem neural integrator supporting the oculomotor system). A Kreisselmeier-type adaptive internal model design was used to model the optokinetic system in [42]. Another variant of the adaptive internal model is [43] whose relevance in modeling the flocculus was explored in [27], [28].

Regarding the plausibility of the reflex adaptation law (8), it corresponds to the schematic model of VOR adaptation in Fig. 2 of [44]. Note, however, [44] does not include the computations of the cerebellum; hence the need for further model development, as done here.

V. CONCLUSION

We have developed a framework for long-term adaptation of reflexes using internal models, inspired by the Miles-Lisberger hypothesis and providing a layer of robustness to brief impulsive disturbances not available with standard adaptive regulator designs. A key idea is that the cost of disturbance rejection by the internal model forms an error signal driving the slow adaptation of reflex gains. A number of movement disorders are associated with failure of the cerebellum to appropriately adapt reflexes [45]; we hope our new model can facilitate the study of such disorders. A second application is development of next generation adaptive robots. Currently reflexes using joint torque sensors are trained with a human in the loop [46]. A next step in the research is to develop a two timescale disturbance rejection framework for Euler-Lagrange models in order to model reflexes of the limbs.

REFERENCES

[1] M. Bodson, A. Sacks, and P. Khosla, "Harmonic generation in adaptive feedforward cancellation schemes," *IEEE Trans. Autom. Control*, vol. 39, no. 9, pp. 1939–1944, Sep. 1994.
[2] W. Messner and M. Bodson, "Design of adaptive feedforward algorithms using internal model equivalence," *Int. J. Adaptive Control Signal Process.*, vol. 9, pp. 199–212, 1995.
[3] S. Pigg and M. Bodson, "Adaptive algorithms for the rejection of sinusoidal disturbances acting on unknown plants," *IEEE Trans. Control Syst. Technol.*, vol. 18, no. 4, pp. 822–836, Jul. 2010.
[4] Y. Wang, G. Pin, A. Serrani, and T. Parisini, "Removing SPR-like conditions in adaptive feedforward control of uncertain systems," *IEEE Trans. Autom. Control*, vol. 65, no. 6, pp. 2309–2324, Jun. 2020.
[5] M. Bodson, "Rejection of periodic disturbances of unknown and time-varying frequency," *Int. J. Adaptive Control Signal Process.*, vol. 19, no. 2/3, pp. 67–88, 2005.
[6] M. Bodson and S. Douglas, "Adaptive algorithms for the rejection of sinusoidal disturbances with unknown frequency," *Automatica*, vol. 33, no. 12, pp. 2213–2221, 1997.
[7] L. Marconi and A. Isidori, "Mixed internal model-based and feedforward control for robust tracking in nonlinear systems," *Automatica*, vol. 36, no. 7, pp. 993–1000, 2000.
[8] R. Marino and P. Tomei, "Disturbance cancellation for linear systems by adaptive internal models," *Automatica*, vol. 49, no. 5, pp. 1494–1500, 2013.
[9] K. Yamamoto, T. Yamamoto, H. Ohmori, and A. Sano, "Adaptive feedforward control algorithms for active vibration control of tall structures," in *Proc. IEEE Int. Conf. Control Appl.*, 1997, pp. 736–742.

[10] F. Aghili and M. Namvar, "Adaptive control of manipulators using uncalibrated joint-torque sensing," *IEEE Trans. Robot.*, vol. 22, no. 4, pp. 854–860, Aug. 2006.
[11] W. MacKay and J. Murphy, "Cerebellar modulation of reflex gain," *Prog. Neurobiol.*, vol. 13, no. 4, pp. 361–417, 1979.
[12] T.-B. Airimitoaie, I. Landau, R. Melendez, and L. Dugard, "Algorithms for adaptive feedforward noise attenuation–A unified approach and experimental evaluation," *IEEE Trans. Control Syst. Technol.*, vol. 29, no. 5, pp. 1850–1862, Sep. 2021.
[13] K. B. Ariyur and M. Krstic, "Feedback attenuation and adaptive cancellation of blade vortex interaction on a helicopter blade element," *IEEE Trans. Control Syst. Technol.*, vol. 7, no. 5, pp. 596–605, Sep. 1999.
[14] M. Bodson, J. S. Jensen, and S. C. Douglas, "Active noise control for periodic disturbances," *IEEE Trans. Control Syst. Technol.*, vol. 9, no. 1, pp. 200–205, Jan. 2001.
[15] S. M. Kuo and D. R. Morgan, "Active noise control: A tutorial review," *Proc. IEEE*, vol. 87, no. 6, pp. 943–973, Jun. 1999.
[16] G. Hillerstrom, "Adaptive suppression of vibrations — A repetitive control approach," *IEEE Trans. Control Syst. Technol.*, vol. 4, no. 1, pp. 72–78, Jan. 1996.
[17] I. Landau, T. Airimitoaie, A. Castellanos-Silva, and A. Constantinescu, *Adaptive and Robust Active Vibration Control*. Berlin, Germany: Springer, 2017.
[18] K. K. Chew and M. Tomizuka, "Digital control of repetitive errors in disk drive systems," *IEEE Control Syst. Mag.*, vol. 10, no. 1, pp. 16–19, Jan. 1990.
[19] H. Basturk and M. Krstic, "Adaptive wave cancellation by acceleration feedback for ramp-connected air cushion-actuated surface effect ships," *Automatica*, vol. 49, no. 9, pp. 2591–2602, 2013.
[20] I. Houtzager, J. -W. van Wingerden, and M. Verhaegen, "Rejection of periodic wind disturbances on a smart rotor test section using lifted repetitive control," *IEEE Trans. Control Syst. Technol.*, vol. 21, no. 2, pp. 347–359, Mar. 2013.
[21] J. Glover, "Adaptive noise cancelling applied to sinusoidal interferences," *IEEE Trans. Acoust. Speech Signal Process.*, vol. 25, no. 6, pp. 484–491, Dec. 1977.
[22] G. Fedele and A. Ferrise, "On the uncertainty on the phase of a stable linear system in the periodic disturbance cancellation problem," *IEEE Trans. Autom. Control*, vol. 61, no. 9, pp. 2720–2726, Sep. 2016.
[23] R. Marino and P. Tomei, "Adaptive output regulation for minimum-phase systems with unknown relative degree," *Automatica*, vol. 130, 2021, Art. no. 109670.
[24] J. Imura, Y. Yokokonji, T. Yoshikawa, and T. Sugie, "Robust control of robot manipulators based on joint torque sensor information," *Int. J. Robot. Res.*, vol. 13, no. 5, pp. 434–442, 1994.
[25] A. Serrani, "Rejection of harmonic disturbances at the controller input via hybrid adaptive external models," *Automatica*, vol. 42, no. 11, pp. 1977–1985, 2006.
[26] S. Messineo and A. Serrani, "Adaptive feedforward disturbance rejection in nonlinear systems," *Syst. Control Lett.*, vol. 58, pp. 576–583, 2009.
[27] M. E. Broucke, "Adaptive internal model theory of the oculomotor system and the cerebellum," *IEEE Trans. Autom. Control*, vol. 66, no. 11, pp. 5444–5450, Nov. 2021.
[28] M. E. Broucke, "Adaptive internal models in neuroscience," *Found. Trends Syst. Control*, vol. 9, no. 4, pp. 365–550, 2022.
[29] F. Miles and S. Lisberger, "Plasticity in the vestibulo-ocular reflex: A new hypothesis," *Annu. Rev. Neurosci.*, vol. 4, pp. 273–299, 1981.
[30] R. Leigh and D. Zee, *The Neurology of Eye Movements*, 5th ed. London, U.K.: Oxford Univ. Press, 2015.
[31] V. Nikiforov and D. Gerasimov, *Adaptive Regulation*, vol. 491. Berlin, Germany: Springer, 2022.
[32] G. Kreisselmeier, "Adaptive observers with exponential rate of convergence," *IEEE Trans. Autom. Control*, vol. 22, no. 1, pp. 2–8, Feb. 1977.
[33] H. Khalil, *Nonlinear Systems*, 3rd ed. Englewood Cliffs, NJ, USA: Prentice-Hall, 2002.
[34] E. Mejia Uzeda and M. E. Broucke, "Robust parameter adaptation and the μ-modification," *Syst. Control Lett.*, vol. 171, 2023, Art. no. 105416.
[35] S. Sastry and M. Bodson, *Adaptive Control: Stability, Convergence, and Robustness*. Englewood Cliffs, NJ, USA: Prentice-Hall, 1989.
[36] P. Ioannou and J. Sun, *Robust Adaptive Control*. New York, NY, USA: Dover, 2012.
[37] J. K. Hale, *Ordinary Differential Equations*, 2nd ed. Malabar, FL, USA: Kreiger Publishing Company, 1980.
[38] J. Sanders, F. Verhulst, and J. Murdock, *Averaging Methods in Nonlinear Dynamical Systems*, 2nd ed. Berlin, Germany: Springer, 2007.
[39] C. Kassardjian, Y. Tan, J. Chung, R. Heskin, M. Peterson, and D. Broussard, "The site of a motor memory shifts with consolidation," *J. Neurosci.*, vol. 25, no. 35, pp. 7979–7985, 2005.
[40] D. Robinson, "The use of control systems analysis in the neurophysiology of eye movements," *Annu. Rev. Neurosci.*, vol. 4, no. 1, pp. 463–503, 1981.
[41] F. Miles and J. Fuller, "Adaptive plasticity in the vestibulo-oculur responses of the rhesus monkey," *Brain Res.*, vol. 80, pp. 512–516, 1974.
[42] E. Battle and M. E. Broucke, "Adaptive internal models in the optokinetic system," in *Proc. IEEE 60th Conf. Decis. Control*, 2021, pp. 641–648.
[43] A. Serrani, A. Isidori, and L. Marconi, "Semi-global nonlinear output regulation with adaptive internal model," *IEEE Trans. Autom. Control*, vol. 46, no. 8, pp. 1178–1194, Aug. 2001.
[44] S. Lisberger and T. Sejnowski, "Motor learning in a recurrent network model based on the vestibulo-ocular reflex," *Nature*, vol. 360, pp. 159–161, 1992.
[45] T. Popa et al., "Abnormal cerebellar processing of the neck proprioceptive information drives dysfunctions in cervical dystonia," *Sci. Rep.*, vol. 8, 2018, Art. no. 2263.
[46] J. Tieck, S. Weber, T. Stewart, J. Kaiser, A. Roennau, and R. Dillmann, "A spiking network classifies human sEMG signals and triggers finger reflexes on a robotic hand," *Robot. Auton. Syst.*, vol. 131, 2020, Art. no. 103566.

ERICK MEJIA UZEDA (Graduate Student Member, IEEE) received the B.A.Sc. degree in electrical engineering from the University of Toronto, Toronto, ON, Canada, in 2021. He is currently working toward the M.A.Sc. degree in systems control with the University of Toronto. From 2019 to 2020, he was a Software Engineer with Interaptix Augmented Reality, Toronto. His research interests include adaptive control, regulator theory, and applications of control theory to systems neuroscience.

MIREILLE E. BROUCKE (Member, IEEE) received the B.S. degree in electrical engineering from the University of Texas at Austin, Austin, TX, USA, in 1984, and the M.S. and Ph.D. degrees from the University of California, Berkeley, CA, USA, in 1987 and 2000. She has six years industry experience at Integrated Systems, Inc. and several aerospace companies. From 1993 to 1996, she was a Program Manager and Researcher with Partners for Advanced Transportation and Highways, University of California. She is currently a Professor of electrical and computer engineering with the University of Toronto. Her research interest focuses on the application of control theory to systems neuroscience.